Polymer Journal (2020) 52:1077–1083
https://doi.org/10.1038/s41428-020-0361-6

ORIGINAL ARTICLE

Creation of porous polymeric membranes by accumulation of water nanodroplets in a miniemulsion system

Yuuka Fukui[1] · Ryota Fujino[1] · Yusuke Sugaya[1] · Keiji Fujimoto[1]

Received: 12 February 2020 / Revised: 11 April 2020 / Accepted: 22 April 2020 / Published online: 25 May 2020

Abstract

We developed a miniemulsion templating method to prepare porous polymeric membranes. First, water nanodroplets were suspended in an oil phase by using a nonionic and polymeric surfactant to form a water-in-oil (*W/O*) miniemulsion. After the nanodroplets accumulated by centrifugation, a small amount of monomer was added as an oil phase to resuspend the water nanodroplets in a monomer phase. Then, photopolymerization of the monomer phase was conducted to generate pores in the polymeric matrix. The size of the nanodroplets was tuned by the surfactant concentration to control the pore size of the membranes. We could produce pore morphologies such as closed-cellular, open-cellular, and bicontinuous structures by tuning the volume fraction of the nanodroplets. Alternatively, nanodroplets were accumulated by centrifugation, and then further surfactants were added to the monomer to suppress the coalescence of nanodroplets. This enabled us to generate a highly porous open-cellular structure while maintaining the size and spherical shape. Next, $HAuCl_4$ was reduced by using the surfactant displayed at the inner surface of the pore wall as the reducing agent. Gold nanoparticles were produced in the inner pores of the polymeric membrane, showing coloration derived from local surface plasmon resonance.

Introduction

There has been an increasing demand for the creation of porous structures owing to their intriguing features, such as a high specific surface area, low weight, thermal insulation, and selective permeation. There have been many approaches to create porous structures, such as interfacial polymerization, phase inversion, porogen incorporation, and templating [1–4]. We focused on the templating approach, which is based on the assembly of sacrificial colloidal templates such as air bubbles, liquid droplets, organic solid particles and inorganic solid particles [5] and subsequent solidification of the outer medium. Among these templates, the emulsion template method has attracted significant interest due to its simplicity and ease because the liquid template can form a variety of shapes, such as interconnected structures, and can be easily removed by a drying process [6–8]. Luo et al. employed a water droplet in a water-in-oil (*W/O*) miniemulsion as a template in which submicron-sized water droplets were dispersed in the suspended oil phase. They carried out emulsification in high aqueous phase fractions of more than 40% and obtained a polymer membrane with pores of ~300 nm, which was consistent with the droplet size [9]. Here, we intended to tune the pore sizes and their morphologies. To obtain a high aqueous phase fraction, we employed centrifugal condensation of water nanodroplets. We previously found that water nanodroplets could maintain their size and shape without any disruption even after centrifugal condensation. Therefore, we utilized the condensed *W/O* miniemulsion as a template to generate a variety of porous structures in the polymeric membrane (Scheme 1a). To stabilize water nanodroplets without causing any size change or phase separation during repetitive centrifugation, decantation, resuspension and polymerization, it was necessary to prevent the diffusion degradation of nanodroplets derived from Ostwald ripening and the coalescence caused by the collision of nanodroplets [10, 11]. Therefore, we attempted to stabilize water nanodroplets in the *W/O* miniemulsion by

Supplementary information The online version of this article (https://doi.org/10.1038/s41428-020-0361-6) contains supplementary material, which is available to authorized users.

✉ Keiji Fujimoto
fujimoto@applc.keio.ac.jp

[1] The Center for Chemical Biology, School of Fundamental Science and Technology, Graduate School of Science and Technology, Keio University, 3-14-1 Hiyoshi, Kohoku-ku, Yokohama 223-8522, Japan

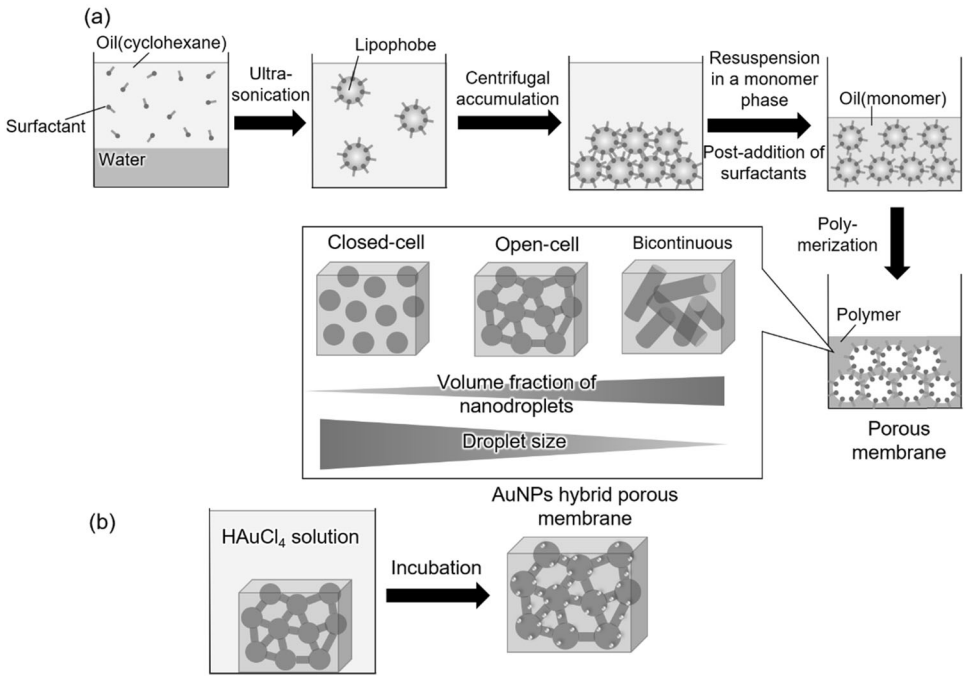

Scheme 1 Schematic illustration of the preparation of hybrid porous membranes by the *W/O* miniemulsion templating method. First, centrifugal accumulation of nanodroplets and subsequent polymerization of the oil phase were carried out to form porous membranes (**a**). Conjugation of gold nanoparticles over the inner pore walls was carried out by utilizing the reducing ability of surfactants

selecting a surfactant and a lipophobe and tuning their amounts. Then, water nanodroplets were accumulated via centrifugation, and subsequently, the oil phase was removed to obtain the condensed miniemulsion (Scheme 1a). After removal of the oil phase, the accumulated nanodroplets were resuspended in a small amount of the monomer to generate a highly concentrated miniemulsion. Then, polymerization of the monomer phase was carried out by UV irradiation, resulting in the formation of polymeric membranes, including water nanodroplets. In this approach, the size of the nanodroplets and their volume fraction (the volume ratio of water nanodroplets to monomers) are thought to be important factors to determine the porous structures, as they are related to the packing density of droplet templates. Therefore, we intended to control the pore morphologies from a closed cell to an open cell by changing these factors. We previously reported that the postaddition of surfactants was an effective way to stabilize the nanodroplets against fusion [12]. Thus, we employed the postaddition of surfactants to maintain the size and morphology of nanodroplets during polymerization.

Chemical modifications of the inner pore surface of the monolith with open cells have been reported to endow the porous membrane with functions such as surface wettability and permeability [13, 14]. Here, we focused on the functionality of surfactant molecules that are displayed at the inner surface of the resultant pores. Thus, we intended to chemically modify the inner walls of porous structures by surface chemistry with respect to the surfactants. Here, we aimed to produce gold nanoparticles (AuNPs) by using the reducing ability of the surfactant containing polyethylene glycol moieties (Scheme 1b). Surface decoration of pores with metal nanoparticles [15, 16] such as AuNPs [17–19] is attractive due to the catalytic properties of these materials and the coloration derived from the porous structure and localized surface plasmon resonance (LSPR) of AuNPs. We attempted to generate AuNPs over the inner pore surface by immersing the porous membranes in a $HAuCl_4$ aqueous solution. We characterized the formation of AuNPs in the inner surface of a porous membrane and its coloration derived from LSPR of AuNPs.

Materials and methods/experimental procedure

Materials

Cyclohexane, calcium nitrate ($Ca(NO_3)_2$) and 1-hydroxycyclohexylphenylketone (Irgacure 184) were purchased from FUJIFILM Wako Pure Chemical Co. (Tokyo, Japan) and used as received. Methyl methacrylate (MMA) was also purchased from Wako Pure Chemical Co. and purified by liquid/liquid extraction prior to use. Ethylene glycol dimethacrylate (EGDMA), *n*-butyl methacrylate (BMA), and 2-ethylhexyl methacrylate (EHMA) were purchased from Tokyo Chemical Industry Co., Ltd (Tokyo, Japan) and used without further purification. The polymeric nonionic surfactant (dimethicone, ABIL EM-90) was obtained from Evonik Industries AG (Essen, Germany) and used without further purification. The water used in all experiments was prepared in a water purification system (WT-100, Yamato

Scientific Inc., Tokyo, Japan) and had a resistivity higher than 18.2 MΩcm.

Preparation and accumulation of water nanodroplets

A *W/O* miniemulsion was prepared in the same manner as described in our previous work [20]. In brief, dimethicone (0.1, 0.15, 0.2, 0.25, 0.5, 0.75, or 1.0 g) was dissolved as a nonionic surfactant in cyclohexane (12.5 g) to prepare an oil phase. To this solution, an aqueous solution (1.5 g) containing $Ca(NO_3)_2$ (0, 5, 10, 100, or 200 mM) was added. This mixture was stirred for 1 h to produce a macroemulsion, followed by ultrasonication (Ultrasonic homogenizer VP-305, 200 W) for 10 min under ice cooling to produce the *W/O* miniemulsion. The hydrodynamic diameters (D_h) and zeta potentials of nanodroplets were measured by using a Malvern Zetasizer Nano-ZS (Malvern Instruments Ltd, Worcestershire, UK).

Preparation and characterization of the porous membranes

The monomer phase was prepared by mixing 1 mL of MMA with 5–150 µL of EGDMA, followed by the addition of 5 wt% Irgacure 184 as a photoinitiator. Then, 1 mL of the *W/O* miniemulsion was centrifuged at 15000 r.p.m. to accumulate nanodroplets containing 200 mM $Ca(NO_3)_2$, followed by the removal of the oil phase. Then, 1000, 600, 400, 300, 200, 150, and 100 µL of the monomer phase was added to the accumulated nanodroplets to set the volume fraction of nanodroplets to 8, 13, 18, 22, 30, 36, and 46 vol%, respectively, and the nanodroplets were resuspended in the monomer phase by simple stirring. Thereafter, photoirradiation (365 nm) was conducted to polymerize the monomer phase, and the samples were left to dry under ambient atmosphere. The morphologies of the resultant porous membranes were observed with a scanning electron microscope (SEM, S-4700, Hitachi, Tokyo, Japan). Prior to SEM observations, all the samples were sputter coated with Os by utilizing an ion sputter (Neoc-Pro, Meiwafosis Co., Ltd Tokyo, Japan). The average pore size was estimated by measuring the diameter of pores in SEM images using ImageJ software. To demonstrate the interconnectivity of the porous structures, the membranes were immersed in toluene with a refractive index of 1.49, which is equivalent to that of PMAA (1.49).

In situ formation of gold nanoparticles on the inner surface of the porous membrane

AuNPs were produced on the pore surface of the membrane with the open-cellular structure, which was prepared with 30 vol% nanodroplets ($D_h = 200 \pm 72$ nm) as follows. First, the surface layer of the membrane was scraped with sandpaper to expose inner pores. After the membrane was treated by permeating ethanol and then water into the pores, it was immersed in a 0.1, 1, or 5 mM $HAuCl_4$ aqueous solution, and incubation was carried out for 3, 8, 20, or 24 h to allow the in situ formation of AuNPs. The resultant AuNP hybrid porous membranes were rinsed with ethanol and then with Milli-Q water. They were immersed in toluene to reduce light scattering by refractive index matching, and then their absorption spectra were obtained by UV–Vis absorption spectroscopy (UV-1800, Shimadzu corporation, Kyoto, Japan).

Results and discussion

Preparation and accumulation of water nanodroplets

As cyclohexane has a high viscosity relative to various organic solvents, it was used as an oil phase to prevent coalescence of nanodroplets through diffusion. $Ca(NO_3)_2$ was added as a costabilizer (lipophobe) inside water nanodroplets to stabilize the *W/O* miniemulsion [12, 20, 21]. According to our previous report [10], dimethicone was used as a surfactant, which is a nonionic polymeric surfactant composed of the main chain of polydimethylsiloxane and the graft chains of hydrophilic polyethylene oxide and hydrophobic polypropylene. To prevent water nanodroplets from coalescing and undergoing Ostwald ripening, it is crucial to modulate the ratio of water and oil and the concentrations of the surfactant and the lipophobe. For instance, submicron-sized nanodroplets ($D_h = 200 \pm 72$ nm) were obtained according to our previous work, where the water and oil ratio was set to 1.5 g/12.5 g in the presence of 0.5 g dimethicone. First, we investigated the effect of the concentration of $Ca(NO_3)_2$ on the stabilization of water nanodroplets in the *W/O* miniemulsion. At $Ca(NO_3)_2$ concentrations higher than 100 mM, we obtained stable nanodroplets (Table. S1). This is because the lipophobe would exert osmotic pressure to counteract the diffusion of water molecules from small nanodroplets to large ones through the oil phase (Ostwald ripening). Next, we centrifuged the *W/O* miniemulsion for the accumulation of nanodroplets. When nanodroplets containing 100 mM $Ca(NO_3)_2$ were incubated for 24 h at 25 °C after centrifugation, their size distribution became polydisperse due to coalescence and Ostwald ripening. Nanodroplets containing 200 mM $Ca(NO_3)_2$ remained the same size ($D_h = 182 \pm 52$ nm) even after solvent replacement, the addition of a monomer phase and redispersion. Furthermore, we aimed to tune the nanodroplet size by the surfactant concentration in the presence of 200 mM $Ca(NO_3)_2$ [10, 22].

It was expected that the number of nanodroplets would increase and the total interface area would be larger when the nanodroplet size decreased. As shown in Table 1, the size of the nanodroplets decreased from ~300 to 190 nm upon increasing the surfactant concentration. This strongly suggests that the small nanodroplets could be stabilized by the surfactants. When the amount of the surfactant was 0.5 g, the nanodroplet size did not significantly increase after the centrifugation and redispersion processes (data not shown). As shown in Table 2, accumulated nanodroplets could be resuspended in various types of monomers without causing phase separation to generate the condensed miniemulsion of water nanodroplets.

Preparation and characterization of the porous membranes

We intended to prepare a porous membrane by using nanodroplets as a template. Water nanodroplets containing 200 mM $Ca(NO_3)_2$ were concentrated to obtain a white precipitate by their accumulation via centrifugation. Then, the supernatant cyclohexane including dimethicone was replaced with a predetermined amount of the monomer mixture of MMA and EGDMA. Water nanodroplets were resuspended in the monomer phase by stirring to generate a milky emulsion with 30 wt% nanodroplets ($D_h = 213 \pm 67$ nm). Next, photoirradiation was conducted to polymerize the monomer phase containing nanodroplets, which were left to dry for water evaporation. Table S2 shows SEM images of porous membranes prepared by polymerization of MMA and EGDMA with different amounts of EGDMA. Nanosized and spherical pores derived from nanodroplets could be observed in the presence of 100 μL of EGDMA, whereas the network structure of microsized pores was formed when the amount of EGDMA was below 50 μL. This is probably because rapid cross-linking of the oil phase could cause an increase in the viscosity of the oil phase to prevent water nanodroplets from fusion and coalescence. In addition, the volume fraction of water nanodroplets is one of the dominant factors in determining the membrane porosity and pore morphology. Table 3 shows SEM images of polymeric membranes prepared by polymerization of the monomer phase at different volume fractions of water nanodroplets. When the volume fraction of nanodroplets was in the range of 8–13 vol%, closed-cellular structures, which were composed of clusters of pores, were generated in the membrane, probably because of the agglomeration of nanodroplets during polymerization. On the other hand, we observed the formation of monolith structures with open cells where the spherical shape of pores was retained when the volume fraction was 18–30 vol%. This is probably because the clusters of pores could be partially fused to connect each pore. Furthermore, when the volume fraction of nanodroplets was increased to 36 and 46 vol%, the pores seemed to be enlarged due to the coalescence of nanodroplets, and their spherical shapes completely disappeared to form bicontinuous structures. To test the connectivity of these obtained membranes, they were immersed in toluene, which has a refractive index similar to that of PMMA. The photographs revealed that the membrane prepared at the volume fraction of 8 vol% was opaque, suggesting that the pores were closed and thereby the immersion of toluene was blocked (Table 4). When the membrane was prepared at a volume fraction of 30 vol%, it was found that the membrane with the interconnected network structures became transparent. This is because the light scattering could be suppressed by filling the pores with toluene. In addition, we studied the effect of the nanodroplet size, which could be tuned by changing the surfactant concentration (Table 1), on the morphology of porous membranes. As seen clearly from Table 5, the pore size was commensurate with the size of

Table 1 Change in the hydrodynamic diameter of nanodroplets by increasing the surfactant (dimethicone) concentration ($Ca^{2+} = 200$ mM)

Amount of surfactant/g	D_h before centrifugation/nm	D_h after centrifugation/nm
0.10	301 ± 158	311 ± 150
0.25	211 ± 83	222 ± 87
0.50	200 ± 72	182 ± 52
1.00	187 ± 56	189 ± 54

Table 2 Photographs showing the *W/O* miniemulsion prepared by centrifugal accumulation and redispersion of nanodroplets in various monomers

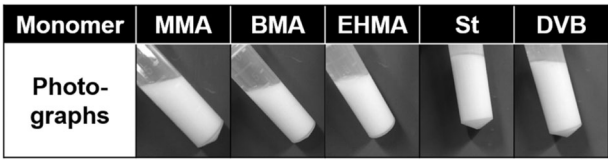

Table 3 SEM images of porous membranes prepared with different volume fractions of nanodroplets ($Ca^{2+} = 200$ mM, dimethicone = 0.5 g)

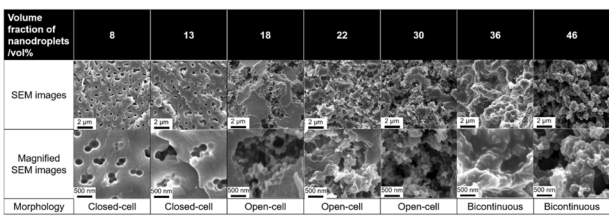

the nanodroplet templates, although the pores tended to be fused as the nanodroplet became large. We could also generate a series of porous membranes by varying the volume fraction of these nanodroplets (Tables S3–S6).

The morphologies of the obtained porous structure are summarized in terms of the relationship between the SEM images and the experimental conditions, such as the volume fraction of nanodroplets and the nanodroplet size (Fig. 1). Closed-cellular structures can be obtained in the low volume fraction of nanodroplets, whereas open-cellular structures are formed in the high volume fraction, and bicontinuous structures appear in the higher volume fraction. It is noteworthy that the bicontinuous structures can be formed in the lower volume fraction as the droplet diameter decreases (~190 nm). According to the literature [9], the average distance between nanodroplets decreases with decreasing droplet size and increasing volume fraction of nanodroplets. We suppose that this could facilitate coalescence of nanodroplets to form the interconnected structure through their fusion during polymerization. This coincides with our previous result, where the decrease in the droplet size enhanced the rate of coalescence between nanodroplets [12]. It is possible to suppress the coalescence of nanodroplets by the postaddition of surfactants to accumulate nanodroplets after centrifugation according to our previous work [12]. Without the postaddition of surfactants, bicontinuous structures could be obtained from 30 vol% nanodroplets ($D_h = 187 \pm 56$ nm) (Table 6, left), where almost all pores were fused and interconnected. On the other hand, a highly porous open-cellular structure could be obtained while maintaining the spherical shape and the size of the nanodroplets by postaddition of surfactants after centrifugation of the nanodroplets (Table 6, right). In this regard, we found that the postaddition method was an effective way to retain the size and shape of nanodroplets, even when they were highly concentrated.

Table 4 Photographs of the closed-cellular (left) and open-cellular porous structures (right) before and after immersion in toluene. The closed-cellular and open-cellular porous structures were generated with 8 and 30 vol% nanodroplets ($Ca^{2+} = 200$ mM, dimethicone = 0.5 g), respectively

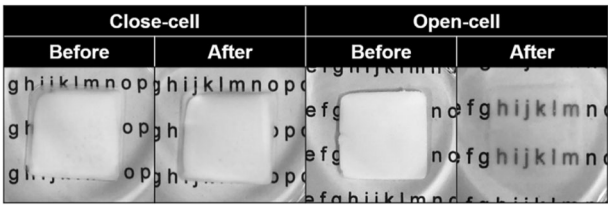

Table 5 SEM observations of closed-cell porous membranes prepared with different amounts of surfactants to produce nanodroplets

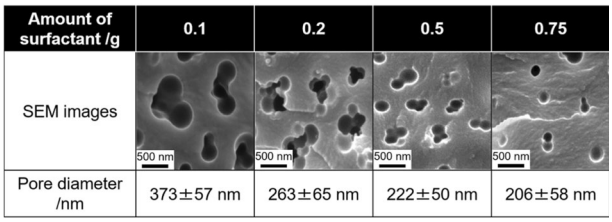

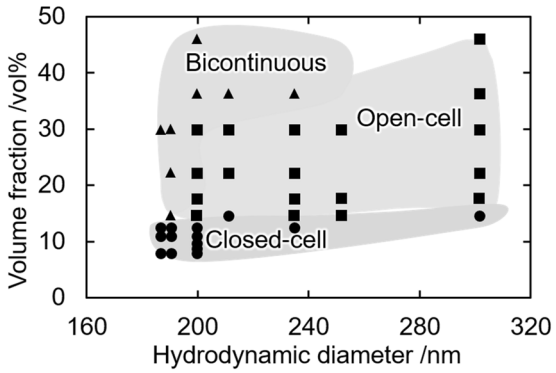

Fig. 1 Experimental diagram showing the effect of the size and volume fraction of nanodroplets on the morphology of porous membranes. The triangle, rectangle, and circle plots show bicontinuous, open-cellular, and closed-cellular structures, respectively

Inner-surface modification of the porous membranes

Next, we intended to carry out chemical modification to endow the inner surface of pores with functionalities. The *W/O* miniemulsion templating method makes it possible to display the surfactant molecules on the inner walls of

Table 6 SEM observations of porous membranes prepared with 30 vol% nanodroplets ($D_h = 187 \pm 56$ nm) before and after the addition of surfactants

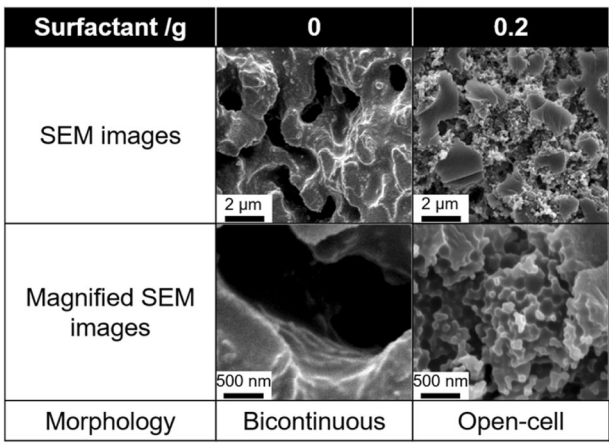

the pores. Dimethicone, used as a surfactant, is expected to possess a reducing ability derived from hydroxy groups in polyethylene glycol branches. This is often utilized to produce metal nanoparticles through reduction of the metal ions [23, 24]. Therefore, we intended to develop a hybrid porous membrane via the generation of metal nanoparticles at the inner walls with the aid of surfactants. Metal nanoparticles possess intriguing properties, such as optical properties associated with their LSPR, conductivity, and catalytic activity. Therefore, the conjugation of metal nanoparticles to porous membranes would be advantageous for various applications, such as color filters, sensors and catalysts. Prior to the pore wall modification, the *W/O* miniemulsion was generated by using dimethicone, and its reducing ability was confirmed by the formation of AuNPs inside the nanodroplets. Table S7 shows photographs of miniemulsions containing $HAuCl_4$ inside the nanodroplets. The emulsion began to turn purple due to the LSPR effect of AuNPs after the emulsification process, and the color became more prominent with time. It was also found that the color was enhanced by increasing the surfactant concentration. These results suggest that AuNPs were formed and grown inside nanodroplets owing to the reducing ability of dimethicone. As illustrated in Scheme 1b, the as-synthesized open-cellular membrane was immersed in $HAuCl_4$ aqueous solution to produce AuNPs. Though it was first opaque, it gradually turned pink, and this color became prominent with time. The color remained the same even after rinsing with ethanol and water, suggesting that AuNPs were stably immobilized on the hybrid porous membrane. To make this color clear, the resultant membrane was immersed in toluene to eliminate the effect of light scattering. As shown in Fig. 2a, the membrane exhibited a deep purple color ascribed to the LSPR of AuNPs. The absorbance increased with the incubation period together with a slight redshift in the peak from 556 to 565 nm after 24 h (Fig. 2b). It is known that the maximum absorption peak tends to redshift with an increase in the size or clustering of AuNPs. An increase in absorbance was also observed by increasing the $HAuCl_4$ concentration (Fig. 2c). These results indicate that both the number and size of AuNPs gradually increased inside the pores because of the reducing ability of the surfactants. In this way, we could achieve surface metal modification of porous membranes by taking advantage of the reactivity of the surfactants displayed on the pore inner wall. In the future, we should accumulate more information on the size, morphology and distribution of AuNPs in the composites, especially with SEM and TEM observations of the cross-section of hybrid porous membranes.

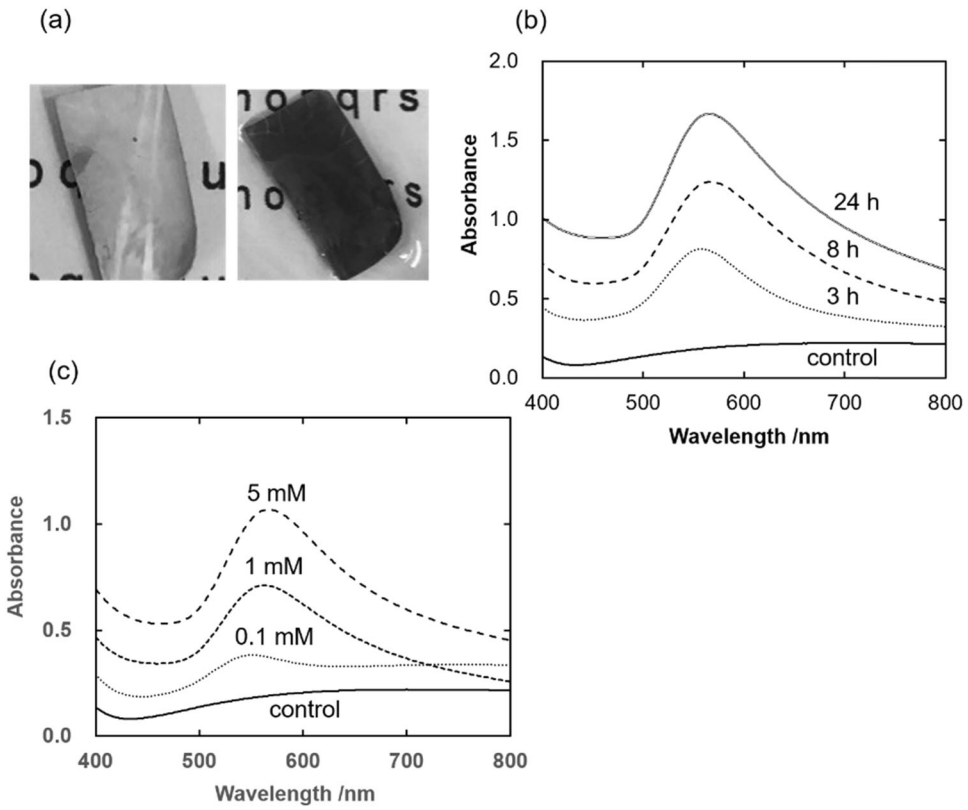

Fig. 2 Photographs of AuNP hybrid porous membranes prepared by immersion in 5 mM $HAuCl_4$ aqueous solution for 24 h in water (left in **a**) and toluene (right in **a**). Effects of the reaction period (5 mM $HAuCl_4$) (**b**) and the concentration of $HAuCl_4$ (20 h) (**c**) on UV–Vis absorption of AuNP hybrid porous membranes in toluene

Conclusions

Nanodroplets containing calcium ions could accumulate via centrifugation in *W/O* miniemulsions. Subsequently, cyclohexane in the oil phase was replaced with a mixture of methyl methacrylate (MMA) and a cross-linking agent, ethylene glycol dimethacrylate (EGDMA). Photoirradiation (365 nm) was conducted to polymerize the monomer mixture. We prepared porous membranes with a variety of morphologies (closed cell, open cell, bicontinuous) via the accumulation of water nanodroplets followed by polymerization in the oil phase. In addition to controlling the size of the pores, their morphologies could be controlled from closed cellular to open cellular by tuning the volume fraction and the size of the nanodroplets. This is probably because the nanodroplets were partially fused during polymerization. Furthermore, several pores were completely fused during polymerization to form a bicontinuous structure with increasing volume fraction of nanodroplets. To stabilize the nanodroplets against fusion, postaddition of the surfactants was performed after centrifugation. A highly porous open-cellular structure was obtained while maintaining the size and spherical shape of the nanodroplets. Next, we could produce AuNPs by immersing the as-prepared open-cellular membrane in the $HAuCl_4$ solution. The resultant structure showed coloration, originating from LSPR of AuNPs.

Compliance with ethical standards

Conflict of interest The authors declare that they have no conflict of interest.

Publisher's note Springer Nature remains neutral with regard to jurisdictional claims in published maps and institutional affiliations.

References

1. Wu DC, Xu F, Sun B, Fu RW, He HK, Matyjaszewski K. Design and preparation of porous polymers. Chem Rev. 2012; 112:3959–4015.
2. Okada K, Nandi M, Maruyama J, Oka T, Tsujimoto T, Kondoh K, et al. Fabrication of mesoporous polymer monolith: a template-free approach. Chem Commun. 2011;47:7422–4.
3. Feinle A, Elsaesser MS, Husing N. Sol–gel synthesis of monolithic materials with hierarchical porosity. Chem Soc Rev. 2016;45:3377–99.
4. Burgess IB, Loncar M, Aizenberg J. Structural colour in colourimetric sensors and indicators. J Mater Chem C. 2013; 1:6075–86.
5. Phillips KR, England GT, Sunny S, Shirman E, Shirman T, Vogel N, Aizenberg J. A colloidoscope of colloid-based porous materials and their uses. Chem Soc Rev. 2016;45:281–322.
6. Silverstein MS. PolyHIPEs: recent advances in emulsion-templated porous polymers. Prog Polym Sci. 2014;39:199–234.
7. Zhang T, Sanguramath RA, Israel S, Silverstein MS. Emulsion templating: porous polymers and beyond. Macromolecules. 2019;52:5445–79.
8. Barbetta A, Cameron NR. Morphology and surface area of emulsion-derived (PolyHIPE) solid foams prepared with oil-phase soluble porogenic solvents: Span 80 as surfactant. Macromolecules. 2004;37:3188–201.
9. Luo YW, Wang AN, Gao X. Miniemulsion template polymerization to prepare a sub-micrometer porous polymeric monolith with an inter-connected structure and very high mechanical strength. Soft Matter. 2012;8:7547–51.
10. Antonietti M, Landfester K. Polyreactions in miniemulsions. Prog Polym Sci. 2002;27:689–757.
11. Landfester K. Synthesis of colloidal particles in miniemulsions. Annu Rev Mater Res. 2006;36:231–79.
12. Fukui Y, Takamatsu H, Fujimoto K. Creation of hybrid polymer particles through morphological tuning of CaCO3 crystals in miniemulsion system. Colloids Surf A Physicochemical Eng Asp. 2017;516:1–8.
13. Livshin S, Silverstein MS. Enhancing hydrophilicity in a hydrophobic porous emulsion-templated polyacrylate. J Polym Sci A Polym Chem. 2009;47:4840–5.
14. Lei L, Zhang Q, Shi SX, Zhu SP. Highly porous poly(high internal phase emulsion) membranes with "open-cell" structure and CO_2-switchable wettability used for controlled Oil/Water separation. Langmuir. 2017;33:11936–44.
15. White RJ, Luque R, Budarin VL, Clark JH, Macquarrie DJ. Supported metal nanoparticles on porous materials. Methods and applications. Chem Soc Rev. 2009;38:481–94.
16. Sarkar S, Guibal E, Quignard F, SenGupta AK. Polymer-supported metals and metal oxide nanoparticles: synthesis, characterization, and applications. J Nanoparticle Res. 2012;14:1–24.
17. Ye YL, Jin M, Wan DC. One-pot synthesis of porous monolith-supported gold nanoparticles as an effective recyclable catalyst. J Mater Chem A. 2015;3:13519–25.
18. Liu Y, Guerrouache M, Kebe SI, Carbonnier B, Le Droumaguet B. Gold nanoparticles-supported histamine-grafted monolithic capillaries as efficient microreactors for flow-through reduction of nitro-containing compounds. J Mater Chem A. 2017;5:11805–14.
19. Khalil AM, Georgiadou V, Guerrouache M, Mahouche-Chergui S, Dendrinou-Samara C, Chehimi MM, Carbonnier B. Gold-decorated polymeric monoliths: In-situ vs ex-situ immobilization strategies and flow through catalytic applications towards nitrophenols reduction. Polymer. 2015;77:218–26.
20. Fukui Y, Fujimoto K. Bio-inspired nanoreactor based on a miniemulsion system to create organic-inorganic hybrid nanoparticles and nanofilms. J Mater Chem. 2012;22:3493–9.
21. Capek I. On inverse miniemulsion polymerization of conventional water-soluble monomers. Adv Colloid Interface Sci. 2010; 156:35–61.
22. Landfester K, Willert M, Antonietti M. Preparation of polymer particles in nonaqueous direct and inverse miniemulsions. Macromolecules. 2000;33:2370–6.
23. Li CC, Shuford KL, Chen MH, Lee EJ, Cho SO. A facile polyol route to uniform gold octahedra with tailorable size and their optical properties. ACS Nano. 2008;2:1760–9.
24. Li CC, Shuford KL, Park QH, Cai WP, Li Y, Lee EJ, Cho SO. High-yield synthesis of single-crystalline gold nano-octahedra. Angew Chem Int Ed. 2007;46:3264–8.